J Mater Sci (2010) 45:4229–4235
DOI 10.1007/s10853-010-4518-0

^{11}C-radiolabeling study of nickel modified H-MCM-41 with methanol as a probe molecule

E. Sarkadi-Priboczki · T. Tsoncheva · N. Kumar · D. Yu. Murzin

Received: 16 December 2009 / Accepted: 12 April 2010 / Published online: 22 April 2010

Abstract ^{11}C-radiolabeling technique was applied to characterize nickel and aluminum modified MCM-41 mesoporous materials. On the basis of desorption and catalytic transformations of methanol molecule, which were studied under different exposure of the surface to ^{11}C-labeled and un-labeled methanol, the contributions of various catalytic active sites to methanol conversion was discussed.

Introduction

During the last two decades, the extended family of mesoporous silicas has provided an ever increasing interest in the fields of adsorption, catalysis, medicine, electronics etc. [1–3] because of their high specific surface area and well-developed porous structure of mesopores with tunable size, shape, and topology. It was established that their modification with different metals leads to the creation of different types of catalytic active sites with acidic–basic and redox properties [4, 5]. To date, many contemporary physicochemical techniques have been applied for their characterization, but usually due to the complexity of the system, the relationship between the various types of catalytic sites and the mechanism of multi-route and multi-step catalytic processes is difficult to be understood. In our previous studies, we have demonstrated the applicability of novel ^{11}C-labeling technique to characterize the catalytic sites of iron- or vanadium oxide-modified MCM-41 silica materials [6–8]. The aim of this article was to extend our study over more complex catalytic system, where the catalytic active sites were regulated via simultaneous modification of mesoporous silica MCM-41 matrix with aluminum and nickel species after pretreatment in oxidative and reduction mediums. Methanol was used as a probe molecule due to its well-known flexibility to convert to different reaction routes, such as dehydration to dimethyl ether (DME) or hydrocarbons, formation of methyl formate or dimethoxymethane, or dehydrogenation to CO, CO_2 and methane, depending on the activities of various type of catalytic sites (acidic–basic, redox or both of them) [7]. Novel experimental procedures with selective coverage of different catalytic sites with ^{11}C-labeled and un-labeled methanol were developed to discuss some critical points of the mechanism of methanol conversion on these materials.

E. Sarkadi-Priboczki
Institute of Nuclear Research, Hungarian Academy of Science, Debrecen, Hungary

T. Tsoncheva (✉)
Institute of Organic Chemistry with Centre of Phytochemistry, Bulgarian Academy of Sciences, Sofia, Bulgaria
e-mail: tsoncheva@orgchm.bas.bg

N. Kumar · D. Yu. Murzin
Laboratory of Industrial Chemistry, Process Chemistry Centre, Abo Akademi University, 20500 Turku, Finland

Experimental

Materials

H-MCM-41 mesoporous molecular sieve (Si/Al ratio 20) was synthesized using a method described elsewhere [9, 10]. Ni/H-MCM-41_ox material, containing 5 wt% Ni was prepared by an incipient wetness impregnation of H-MCM-41 with an aqueous solution of nickel nitrate and further calcination at 723 K for 4 h. Ni/H-MCM-41_red material was obtained after reduction of Ni/H-MCM-41_ox at 723 K for 4 h in a flow of hydrogen (10 °C/min). For

comparison, reference MCM-41 silica (Ni/Si-MCM-41, 5 wt% Ni, BET surface area of 922 m^2/g, total pore volume of 0.9 cc/g, and average pore diameter of 3.9 nm) samples were obtained using the procedure described in [11].

The samples were characterized by XRD (diffractometer Philips PW 1800), XPS (PerkinElmer PH1 5400 ESCA system), X-ray fluorescence spectrometer (Siemens SRS 303), N_2-physisorption (Sorptometer 1900, Carlo Erba Instruments), and TPD of hydrogen (Autochem 2910, Micrometrics) [9].

Catalytic experiments

^{11}C-radiolabeling experiments were done in a closed static reactor as described in [12]. Normally, the experiments were started after pre-adsorption of ^{11}C-methanol at 313 K (standard procedure, Scheme 1a). The desorbed ^{11}C-methanol during the subsequent heating of the sample up to 450 K was removed in He and trapped into P_2O_5 for radioactivity measurements. Alternatively, some experiments were carried out using a *consecutive ^{12}C–^{11}C procedure* (shortly denoted as $^{12}C \rightarrow {}^{11}C$), where initially ^{12}C-methanol was adsorbed at 313 K, followed by its partial desorption by heating up to 453 K, and subsequent adsorption of ^{11}C-methanol at 333 or 453 K (procedure 1 and 2, respectively, Scheme 1b). For comparison, reversed order of procedure 1, Scheme 1b (denoted as $^{11}C \rightarrow {}^{12}C$) was also applied for selected investigations. The catalytic activity was measured in the temperature interval of 460–650 K using GC analysis with a flame-ionization (FID) and radio (RD) detectors.

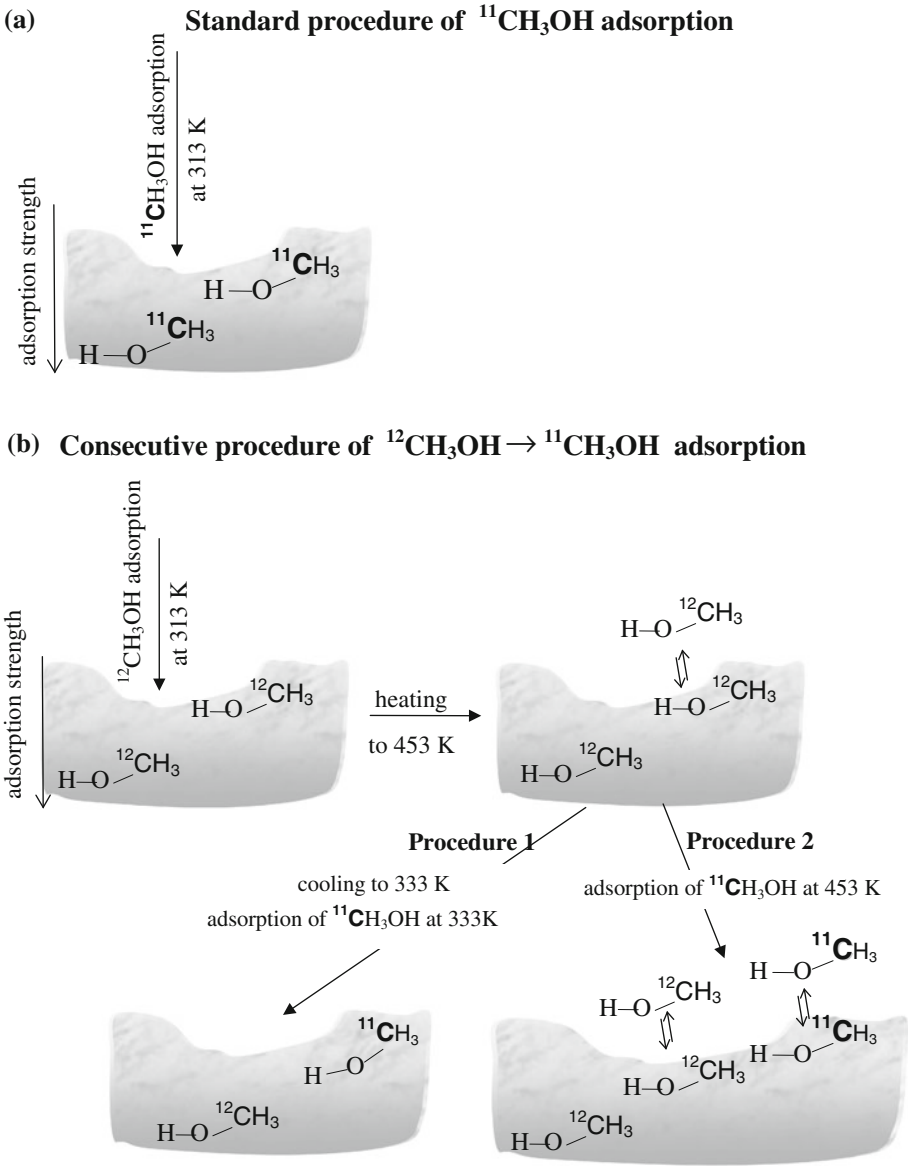

Scheme 1 Standard (**a**) and consecutive (**b**) procedure of ^{12}C–^{11}C-methanol pre-adsorption

Results and discussion

Physicochemical characteristics of the parent, and modified with nickel H-MCM-41 were presented in our previous study [9]. X-ray fluorescent analysis, XRD patterns, and N_2-physisorption measurements confirmed the preparation of high-quality H-MCM-41 mesoporous material with Si/Al ratio of 20, BET surface area of 1214 m^2/g, and average pore diameter of about 1.5 nm. After the modification with Ni, no significant changes in MCM-41 structure were found. The observed decrease of the BET surface area for Ni/H-MCM-41_ox (BET = 1051 m^2/g) could be assigned to the formation of nickel oxide nanoparticles, included in the pore matrix. The formation of larger nickel/nickel oxide nanoparticles (about 9 and 6 nm, respectively), probably located on the outer surface, was also established by XRD for both oxidized and reduced nickel modified MCM-41 materials. TPR measurements showed that about 30% of Ni was in metallic form after the reduction [9]. These data combined with XPS analysis [9] confirm the existence of Ni species in different states, e.g., Ni and Ni-oxide species. For comparison, in the case of reference Ni/Si-MCM-41 sample, no XRD reflections in a wide angle region were obtained, indicating the presence of finely dispersed nickel oxide nanoparticles in it (not shown).

The temperature dependencies of ^{11}C-radioactivity level of the samples after *standard pre-adsorption procedure* with ^{11}C-methanol (Scheme 1a), are presented in Fig. 1a. We expect that, under this pre-adsorption procedure, all catalytic sites were covered with labeled methanol. The observed high level of radioactivity for H-MCM-41, which was also temperature independent, evidences a strong and irreversible adsorption of methanol most probably with the formation of methoxy groups bonded to the surface acid sites [10, 13–15]. The decrease of the radioactivity level for Ni/H-MCM-41_ox and Ni/Si-MCM-41 above 410 K (much pronounced for the former sample) is due to intensive desorption of ^{11}C-methanol from the surface, indicating the presence of weakly adsorbed active sites in the nickel-modified materials. In order to describe different catalytic sites more precisely, the experiments with *consecutive pre-adsorption procedure* was carried out. After the consecutive $^{11}C \rightarrow {}^{12}C$-methanol pre-adsorption, where the coverage of the strongest sites with ^{11}C-methanol is mainly realized (Fig. 1b), a significantly high radioactivity level was observed for the reference Ni/Si-MCM-41 material throughout the temperature interval under investigation. The obtained result indicates a strong adsorption ability of highly dispersed nickel oxide nanoparticles [4, 16, 17]. We should stress on the similarity of the desorption curves for Ni/H-MCM-41 after its pretreatment in reduction and oxidation mediums if a consecutive $^{12}C \rightarrow {}^{11}C$-methanol pre-adsorption procedure, with predominant coverage of the weaker sites with ^{11}C-methanol was carried out (Fig. 1c). Obviously, this experiment illustrates the preservation of these weakly adsorbing sites during the reduction pretreatment, which according to TPR data (see above) could be ascribed to hardly reducible nickel oxide species.

Methanol conversion on different MCM-41 materials according to *standard procedure* of methanol pre-adsorption (Scheme 1a) is shown in Fig. 2. The predominant formation of DME below 553 K for H-MCM-41 (Fig. 2a) clearly indicates the activity of acidic sites [18]. At the same time, lower dehydration activity and a new reaction route on the redox nickel oxide sites leading to the

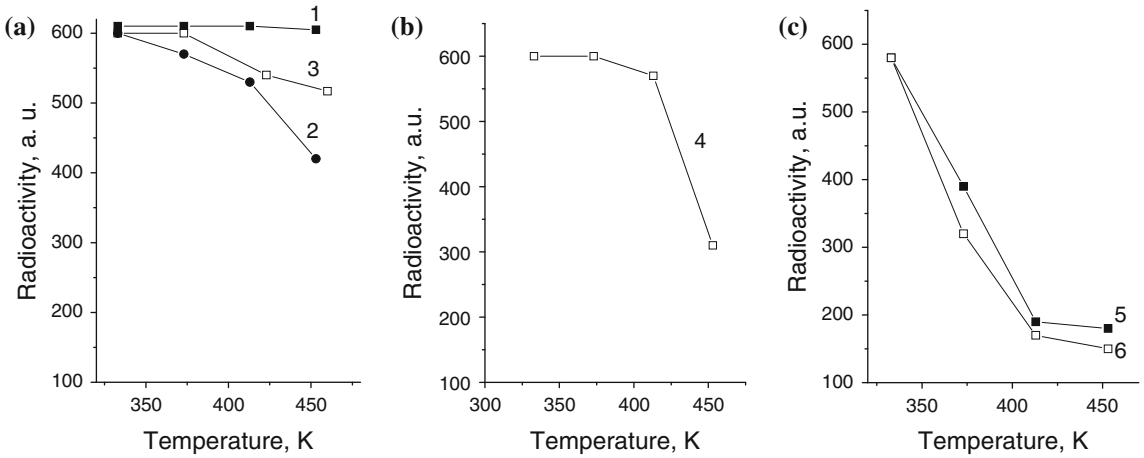

Fig. 1 Desorption of ^{11}C-methanol on various samples after different pre-adsorbing procedures. **a** H-MCM-41 (*1*), Ni/H-MCM-41_ox (*2*), and reduced Ni/Si-MCM-41 silica (*3*) according to standard ^{11}C-methanol adsorption (Scheme 1a). **b** Ni/Si-MCM-41_ox (*4*) after ^{11}C-methanol adsorption at 313 K—its desorption at 453 K followed by ^{12}C-methanol adsorption at 33 3 K (reverse order of procedure 1, Scheme 1b). **c** Ni/H-MCM-41_ox (*5*) and Ni/H-MCM-41_red (*6*) after ^{12}C-methanol adsorption at 313 K, its desorption at 453 K and following ^{11}C-methanol adsorption at 333 K (procedure 1, Scheme 1b)

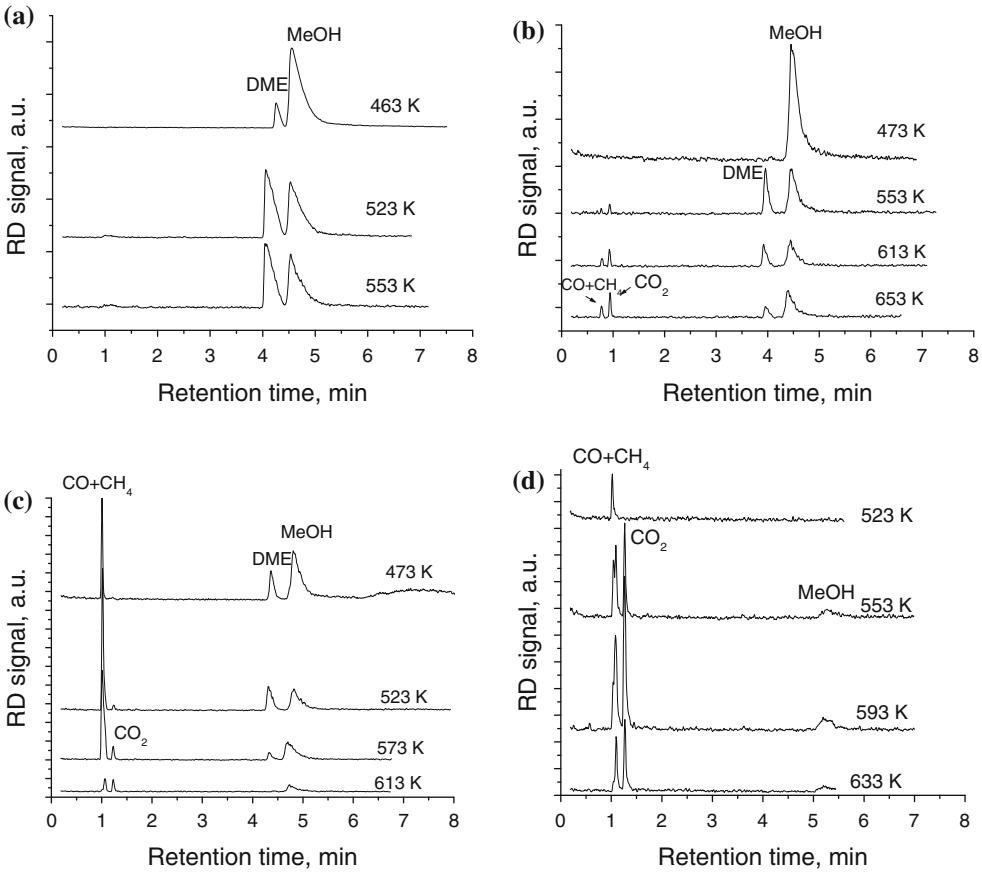

Fig. 2 ^{11}C-methanol conversion on H-MCM-41 (**a**), Ni/H-MCM-41_ox (**b**), Ni/H-MCM-41_red (**c**), and reduced Ni/Si-MCM-41 silica (**d**) after standard adsorption of ^{11}C-methanol

formation of CO, CO_2, and CH_4 even at 553 K are found for Ni/H-MCM-41_ox (Fig. 2b) [4]. Methane is the main product for Ni/H-MCM-41_red (Fig. 2c) indicating the activity of metallic nickel nanoparticles in this sample [17]. This assumption is also well supported with the data for the reduced Ni/Si-MCM-41 material (Fig. 2d), where CO, CO_2, and CH_4 are the only registered products. It is interesting to stress that the dehydration activity of Ni/H-MCM-41_red was higher in comparison with that one of Ni/H-MCM-41_ox, which is probably due to the changes in the environment of the surface Brønsted acid sites during the reduction of nickel species.

When a *consecutive* $^{12}C \rightarrow {}^{11}C$*-methanol pre-adsorption* procedure was carried out (procedure 2, Scheme 1b), a predominant coverage of the strongest sites with ^{12}C-methanol and partial exchange of un-dissociatively adsorbed ^{12}C-methanol molecules with ^{11}C-labeled when they are on the weaker sites is expected. In the present case, lower dehydration activity to DME (Fig. 3a) in comparison with that obtained using the standard pre-adsorption procedure (Fig. 2a) and formation of labeled DME were registered for H-MCM-41. This result confirms a reaction mechanism of DME formation on the weaker sites due to methylation of un-dissociatively adsorbed methanol molecules with surface methoxy intermediates [19, 20 and refs. therein]. At temperatures above 573 K (Fig. 3a), formation of un-labeled hydrocarbons was mainly registered by FID detector, and their amounts remained much higher than those in the labeled products. We should also stress on higher amounts of C_3 and C_4 hydrocarbons, which were found in ^{12}C-products in comparison with ^{11}C-ones. These results evidence the important role of strong Brønsted acid sites for methanol conversion to hydrocarbons, where carbon chain growth mechanism with the participation of surface methoxy species probably via carbene or carbenium ion intermediates [18, 21] could be suggested. It seems that a mechanism with the participation of un-dissociatively bonded to the surface methanol molecules and/or that ones from the gas phase is less probable [22, 23].

At low temperatures, higher activity to DME was detected both by FID and RD detectors for Ni/H-MCM-41_ox (Fig. 3b) in comparison with H-MCM-41 (Fig. 3a). The activity of Lewis acidic sites, which are most probably low coordinated NiO_x species [16], could be assumed for the former material. However, in the case of Ni/H-MCM-41_ox (Fig. 3b) the formation of hydrocarbons was strongly suppressed. According to the desorption experiments (Fig. 1a), the observed effect could be ascribed to a decreased number of the strong Brønsted acidic sites after the modification of H-MCM-41 with nickel oxide species.

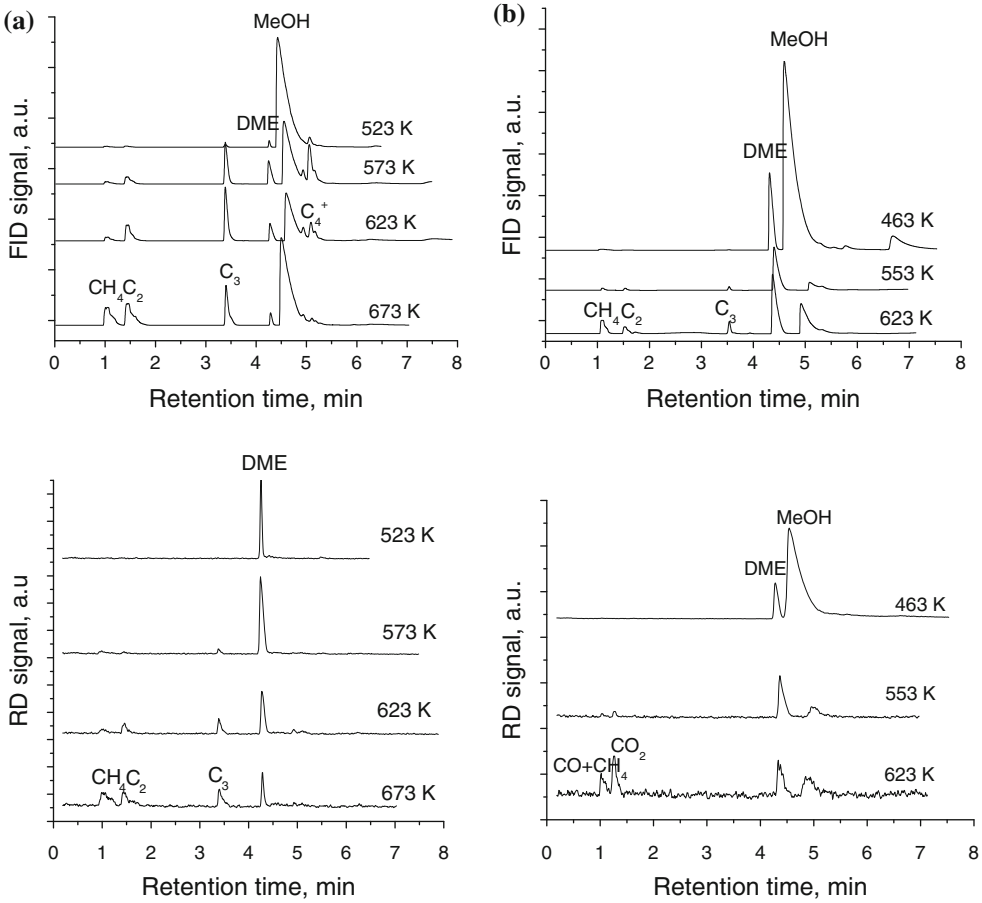

Fig. 3 Methanol conversion after consecutive ^{12}C–^{11}C-methanol adsorption with final ^{11}C-methanol adsorption at 453 K (procedure 2) on H-MCM-41 (**a**), and Ni/H-MCM-41_ox (**b**)

Similar data for Brønsted acidity decrease in H-MCM-41 during its modification with metal/metal oxide species has been reported in [24, 25].

If the experiments were carried out according to the *procedure 1*, Scheme 1b, with final adsorption of ^{11}C-methanol at lower temperature, then the occupation of the weakest adsorption sites predominantly by ^{11}C-methanol could be expected. In this case, among the labeled products (Fig. 4a), a decrease in the dehydration activity to DME without any significant increase of methane and CO_2 formation was found in comparison with the experiment which was carried out according to the *procedure 2,* Scheme 1 (Fig. 3b). It could be due to easier desorption of ^{11}C-methanol weakly bonded to the surface without its further transformation. On the contrary, higher catalytic activity with predominant formation of C_3- and C_4-hydrocarbons was observed by FID detector (Figs. 4a, 3b). This result confirms a mechanism of DME and hydrocarbons formation via methylation of preliminary activated on the catalyst surface methanol molecule [19, 26].

After the reduction of Ni/H-MCM-41_ox, an increase in methanol conversion and formation of DME, CO_2, and methylformate (MF) was registered by RD detector. At the same time, higher activity to DME and hydrocarbons was established during the FID measurements. Therefore, the formations of CO_2 and MF are strongly related to the activity of metallic nickel nanoparticles. However, we should stress on the differences of methane and CO_2 selectivities, which were observed when the experiments were carried out by the *standard* and *consecutive* procedures (Fig. 2c). The extremely high amount of $^{11}CO_2$, which was registered during the latter one, could be an evidence for its formation on weakly adsorbed metallic Ni nanoparticles, where the methanation of CO is strongly suppressed [11]. The observed high CO_2 selectivity in this case confirms a mechanism of its formation via formate intermediates and in a much lower extent—via MF decomposition to CO_2 and methane [4].

Conclusion

Novel ^{11}C-radiolabeled technique is developed to study the role of different catalytic sites of nickel- and aluminum-modified MCM-41 in methanol conversion. The data from desorption and catalytic analysis for Ni/H-MCM-41 strongly indicate a decrease in the strength of Brønsted acidic sites by the influence of nickel oxide species situated

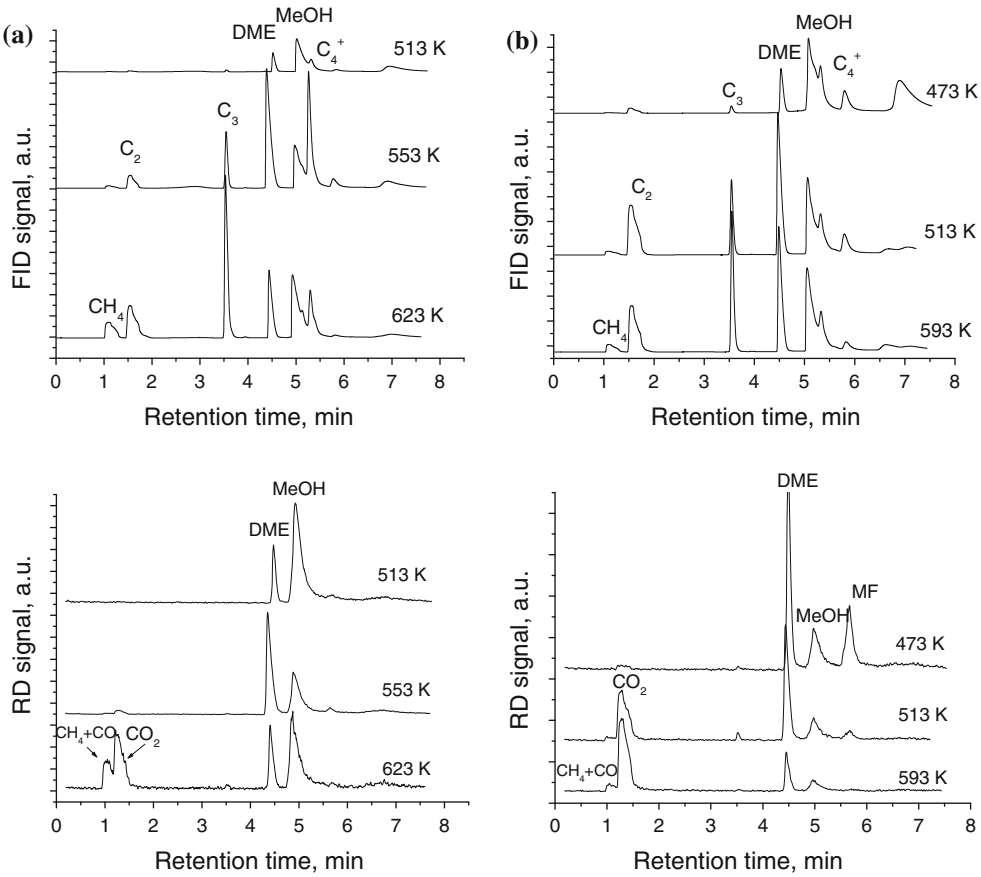

Fig. 4 Methanol conversion after consecutive ^{12}C–^{11}C-methanol adsorption at 313 K and final ^{11}C-methanol adsorption at 333 K (procedure 1) on Ni/H-MCM-4_ox (**a**), and Ni/H-MCM-4_red (**b**)

in their vicinity. A mechanism of DME formation on the weaker sites via methylation of un-dissociativly adsorbed methanol molecules with surface methoxy intermediates is considered. The participation of Lewis acidic sites, which are most probably the low-coordinated NiO_x species, in DME formation is also established. The important role of strong Brønsted acidic sites in methanol conversion to hydrocarbons via carbene or carbenium ion intermediates, but not via participation of un-dissociatively bonded to the surface methanol molecules and/or those from the gas phase, is assumed. CO_2 seems to be formed on the weaker Ni-containing adsorption sites mainly with the participation of surface formate intermediates, and to a much lesser extent, via methylformate.

Acknowledgements Financial supports provided by Bulgarian Academy of Sciences, the Bulgarian-Hungary interacademic exchange, Ministry of Education and Science (project DO 02-184), and by the Hungarian Scientific Research Fund No. T 048345 are gratefully acknowledged.

References

1. Taguchi A, Schüth F (2005) Microporous Mesoporous Mater 77:1
2. Schüth F, Wingen A, Sauer J (2001) Microporous Mesoporous Mater 44–45:465
3. Thu PTT, Thanh TT, Phi HN, Kim SJ, Vo V (2010) J Mater Sci 45:2952. doi:10.1007/s10853-010-4288-8
4. Barteau MA (1996) Chem Rev 96:1413
5. Szegedi A, Popova M, Minchev C (2009) J Mater Sci 44:6710. doi:10.1007/s10853-009-3600-y
6. Sarkadi-Pribóczki E, Tsoncheva T, Ivanova L (2008) Catal Commun 9:1932
7. Sarkadi-Pribóczki E, Tsoncheva T, Ivanova L (2009) Can J Chem 87:478
8. Sarkadi-Pribóczki E, Tsoncheva T (2009) Catal Commun 10:1216
9. Bernas A, Laukkanen P, Kumar N, Arvela PM, Väyrynen J, Laine E, Holmbom B, Salmi T, Murzin DYu (2002) J Catal 210:354
10. Mäki-Arvela P, Kumar N, Kubička D, Nasir A, Heikkilä T, Lehto V-P, Sjöholm R, Salmi T, Murzin DYu (2005) J Mol Catal A Chem 240:72
11. Tsoncheva T, Linden M, Rosenholm J, Minchev C (2005) React Kinet Catal Lett 86(2):275
12. Sarkadi-Priboczki E, Kumar N, Nieminen V, Kovacs Z, Murzin DYu (2007) Catal Lett 114:17
13. Wang W, Buchholz A, Arnold A, Xu M, Hunger M (2003) Chem Phys Lett 370:88
14. Jiang Y, Wang W, Marthala VRR, Huang J, Sulikowski B, Hunger M (2006) J Catal 238:21
15. Anderson MW, Klinowski J (1990) J Am Chem Soc 112:10
16. Ziolek M, Kujawa J, Saur O, Lavalley JC (1993) J Phys Chem 97:9761
17. Mavrikakis M, Barteau MA (1998) J Mol Catal A Chem 131:135
18. Chang CD (1983) Catal Rev Sci Eng 25:1
19. Jiang Y, Hunger M, Wang W (2006) J Am Chem Soc 128:11679

20. Ballarini N, Cavani F, Maselli L, Montaletti A, Passeri S, Scagliarini D, Flego C, Perego C (2007) J Catal 251:423
21. Haw JF, Song W, Marcus DM, Nicholas JB (2003) Acc Chem Res 26:317
22. Arstad B, Kolboe S (2001) J Am Chem Soc 123:8137
23. Seiler M, Wang W, Buchholz A, Hunger M (2003) Catal Lett 88:187
24. Fang K, Wei W, Ren J, Sun Y (2004) Catal Lett 93:235
25. Nieminen V, Kumar N, Salmi T, Murzin DYu (2004) Catal Commun 5:15
26. Forrester TR, Howe RW (1987) J Am Chem Soc 109:5076